Journal of Materials Processing Technology 222 (2015) 148–154

Contents lists available at ScienceDirect

Journal of Materials Processing Technology

journal homepage: www.elsevier.com/locate/jmatprotec

Application of a plate sonotrode to ultrasonic degassing of aluminum melt: Acoustic measurements and feasibility study

D.G. Eskin [a,b,*], K. Al-Helal [a], I. Tzanakis [a]

[a] Brunel University London, Brunel Centre for Advanced Solidification Technology, Uxbridge UB8 3PH, United Kingdom
[b] Tomsk State University, Tomsk 634050, Russia

ARTICLE INFO

Article history:
Received 20 January 2015
Received in revised form 4 March 2015
Accepted 5 March 2015
Available online 13 March 2015

Keywords:
Ultrasound
Cavitation
Degassing
Aluminum
Sonotrode, Acoustic pressure

ABSTRACT

A flat plate sonotrode was used for ultrasonic melt processing (degassing) of aluminum melts. Calculations showed that this sonotrode should have several antinodes with maximum amplitude, spaced at 16.5 mm. The direct measurements of the amplitude in air and indirect measurements of foil cavitation erosion in water validated these calculations. Unique acoustic measurements of cavitation activity in water and a liquid aluminum alloy were performed using a cavitometer and confirmed that the cavitation conditions were met with this scheme. The melt degassing efficiency using the plate sonotrode was significantly higher (70–80%) than with a conventional cylindrical sonotrode (45–50%) in batch operation. The new scheme was also suitable for ultrasonic melt processing in the melt flow giving about 50% degassing efficiency, which opens the way to upscaling this technology to treat larger volumes of melt.

1. Introduction

One of the objectives of good casting technology is to avoid porosity in a casting. This is achieved through melt degassing. In liquid aluminum, the amount of hydrogen can reach 0.3–0.5 cm^3/100 g, while the industrial standard requires the concentration of hydrogen before casting close to 0.1 cm^3/100 g (Waite, 1998). Currently the most adopted technology of degassing is so-called argon rotary degassing where a porous graphite rotor is submerged into the melt and Ar is purged through the rotor to the bottom of the bulk melt. The rotating graphite shaft shears and disperses Ar bubbles that float to the surface, collecting hydrogen dissolved in the melt. Although well established, this technology has some drawbacks such as high dross formation, not recycled expensive Ar, and potential damage of the graphite rotor with subsequent melt contamination.

Ultrasonic degassing is among the first potential applications of acoustic cavitation in liquids. It has been tried on the industrial scale for aluminum melt degassing in foundries and cast houses back in the 1960–1980s and proved to be a clean and robust technology, though requiring some specialty equipment and set-up as reported by Eskin (1965) and recently reviewed by Eskin and Eskin (2014). In recent years the interest to this technology has increased due to its environment friendliness and potential versatility. It has been shown that the amount of hydrogen can be decreased to the levels lower than in the case of Ar degassing with much less dross formation (Eskin et al., 2015).

The mechanism of ultrasonic degassing is rather well understood and a recent overview can be found elsewhere (Eskin and Eskin, 2014). Here we would like to point out the main features. Eskin (1995) reports that ultrasonic cavitation is required to initiate gas bubble formation in the aluminum melt. Although there are no free gas bubbles in the melt (unlike water), Eskin and Eskin (2014) note that there are numerous interfaces such as oxide particles with absorbed atomic hydrogen layer or even molecular hydrogen in inclusion's surface defects that act as cavitation nuclei, significantly decreasing the cavitation threshold, i.e., the pressure required to initiate cavitation in the liquid medium. Kapustina (1970) summarized the mechanisms of ultrasonic degassing by rectified diffusion into a pulsating bubble and Eskin (1995) extended the theory to liquid aluminum. As a bubble oscillates in the alternating sound field, it acts as a pump extracting more and more hydrogen from the melt with each expansion. The bubbles therefore grow and subsequently float to the surface, releasing the hydrogen to the atmosphere. As mentioned by Eskin and Eskin (2014), melt flows created by the ultrasound source (acoustic streaming and secondary flows) facilitate bubbles distribution and, hence, degassing.

A conventional scheme to introduce ultrasonic vibrations into the melt is through a concentrated source, i.e., horn or sonotrode. In this case the sonotrode is submerged into the melt from the top,

* Corresponding author at: Brunel University London, Brunel Centre for Advanced Solidification Technology, Uxbridge UB8 3PH, United Kingdom.
Tel.: +44 1895 265317.
E-mail address: Dmitry.Eskin@brunel.ac.uk (D.G. Eskin).

http://dx.doi.org/10.1016/j.jmatprotec.2015.03.006

creates a cavitation zone underneath and the acoustic streaming is directed downwards, pushing the oscillating cavitation bubbles to the bulk of the melt. The sonotrode should have certain length, multiple of the half-wavelength of longitudinal vibrations of the given frequency in the given sonotrode material. This scheme has been used in most of research and pilot-scale trials, both in the batch operations and in the melt flow (see review in Eskin and Eskin, 2014). As the ultrasonic degassing requires some time to process a certain melt volume, which includes the sonication time proper and some resting time allowing the bubbles to float, increasing the volume in the batch operation or decreasing the processing time in the melt-flow operation needs multiple sonotrodes. The practical experience showed examples of as much as eight sonotrodes used for degassing a commercial-size melt charge (Eskin, 1965). Apparently, this technological scheme has its limitations, especially if one takes into account that each sonotrode requires a separate transducer to excite it.

Another possible scheme for ultrasonic processing of liquids has been suggested by Shoh (1976) for low-temperature liquids and by Eskin (2002) for liquid metals but not intended for degassing. A flat extended plate submerged into the melt and transmitting flexural rather than longitudinal waves gives some obvious advantages. For example, a larger vibrating surface increases the area where the cavitation conditions can be met and cavitation bubble are formed. Therefore, the acoustic wave and cavitation can be transmitted to a larger melt volume. There is also a possibility to position the plate in the lower part of the melt volume with bubble naturally directed upwards, and the possibility to perform ultrasonic processing in the melt flow without obvious limitations of the degassed volume.

This paper describes the evaluation of this scheme in terms of cavitation conditions generated and the feasibility study on the application of a flat plate sonotrode to the ultrasonic degassing of liquid aluminum alloys.

2. Experimental

The experimental setup consisted of a 5-kW ultrasonic generator, a water-cooled 5-kW magnetostrictive transducer, a steel half-wavelength conical concentrator 65 to 40 mm in diameter, a steel half-wavelength extension and a titanium plate sonotrode 40 mm wide, 2 mm thick, and 320 mm in total length (the effective length working in the melt depended on the shape of the plate, i.e., its bending). The working frequency was 17.15 kHz. The plate was attached to the bottom of the extension by a steel stud and nut. Eskin (1965) reports that titanium is not an ideal metallic material for a sonotrode as it eventually dissolves in liquid Al. However, its acoustic characteristics are suitable for ultrasonic applications and the dissolution rate in liquid metal is relatively small for short-term experiments, which is frequently used in lab-scale research. In our case the experiments in liquid aluminum did not exceed 2 min and the amount of dissolved Ti was measured as 0.05 wt%. As the main purpose of the work was degassing and not grain refinement, this small amount of dissolved Ti did not affect the acoustic performance of the sonotrode and the degassing results.

Four types of experiments were performed: (i) in air with the aim to measure the amplitude and wavelength of flexural vibrations in a plate sonotrode, (ii) in water with the aim to measure the acoustic parameters and visualize the cavitation, (iii) in a closed compartment with a liquid A356-type aluminum alloy for degassing and acoustic measurements, and (iv) in an open launder with the flowing melt of the same alloy for degassing.

The vibration amplitude was measured in air using a contactless vibrometer based on a capacitance principle (Eskin and Eskin, 2014). The measuring tip of the vibrometer was placed within 1 mm distance from the vibrating surface. The null-to-peak amplitude was measured in several points along the longitudinal centerline of the plate. Experiments in water were performed in a transparent launder similar in geometry to the launder used for liquid aluminum or in a glass vessel with the dimensions close to those of the degassing chamber (see Fig. 1). Acoustic measurements in water and in the liquid aluminum alloy were taken by a calibrated high-temperature cavitometer (Tzanakis et al., 2015a), and included the frequency spectrum and acoustic pressure. The frequency spectrum was acquired by an external digital oscilloscope (picoscope) attached to the cavitometer. The picoscope allowed real-time signal monitoring of the cavitometer probe's data and ultrasonic parameters. A Blackman window was applied to the raw voltage signal, which was then transformed to the frequency domain with a Fast Fourier Transform. Unless otherwise specified, 30 signal averages of the acquired signal were typically taken using a resolution bandwidth of 95 Hz. The time for this signal acquisition was approximately 30×1.3 (time gate) = 39 ms. Each experiment was repeated to ensure reproducibility of results. The cavitometer probe was made of tungsten and was suitable for temperatures up to 750 °C. During measurements the tip of the cavitometer probe was within 15 mm from the surface of the vibrating plate. The ambient and internal noise level with an idle sonotrode has been taken by the cavitometer and then subtracted from the spectra obtained with the working sonotrode.

The experiments with the liquid aluminum alloy had the main aim of evaluating the degassing efficiency that was taken as the decrease of hydrogen concentration related to the starting hydrogen concentration. Cut ingots from a commercial A356 alloy (7% Si, 0.3% Mg) were melted in a tilting furnace in a clay-graphite crucible. The melt was maintained in the furnace at 740–750 °C or 800 °C. The samples were taken in the furnace before pouring and during the experiment at the end of the launder for the processing in the flow or at the end of degassing from the degassing chamber in the batch operation. Different amounts of aluminum melt were treated as indicated in the corresponding parts of the text. The hydrogen concentration was measured using a standard reduced pressure test (Davies, 1993). In this test the two liquid samples are taken simultaneously from the melt and are solidified, one in air and the other under reduced pressure. In the latter case, the dissolved hydrogen is forced to precipitate from the solidifying metal and form porosity. The densities of the two samples are then determined by the Archimedes method and the ratio of the density difference to the density of the sample solidified in air is taken as so-called density index. It can be subsequently recalculated to the hydrogen concentration using a previously established correlation relationship in which the direct measurements of hydrogen by an Alspec-H analyzer have been used (Eskin et al., 2015). As the hydrogen solubility in liquid aluminum depends on the environment humidity, the measurements have been taken using a weather station. A principal scheme of the experiment in a launder is shown in Fig. 1. The degassing chamber measured 150×100 mm in cross-section and 220 mm in length. In the beginning of the experiment the outlet from the degassing chamber was closed with a plug, as soon as the chamber was filled with the required amount of melt, the sonication started and the plug was taken out, while the melt continued to pour into the chamber. The size of the outlet assured about 2 min of residence time of the melt during ultrasonic degassing. In the case of ultrasonic processing in the melt flow, the melt flow rate was calculated by dividing the weight of the liquid metal by the time required for this melt to pass through the degassing chamber. The flow rate was controlled by the outlet orifice of the degassing chamber. The launder had the width and height at 100 mm and the length 890 mm. The launder had some baffles to slow down the melt flow and allow the bubbles sufficient time to float to the surface, the residence time varied between 1 and 4 min. All parts of the melt transfer system were made of a refractory ceramic board and

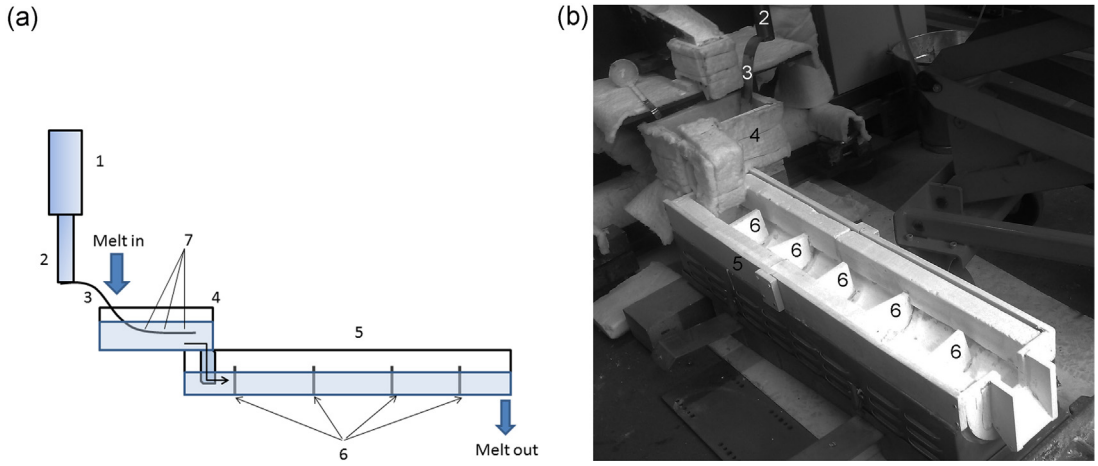

Fig. 1. (a) A scheme of ultrasonic degassing experiment: (1) ultrasonic transducer; (2) concentrator with extension; (3) plate sonotrode; (4) degassing chamber; (5) launder; (6) baffles; and (7) points of acoustic measurements and (b) actual setup for ultrasonic degassing in the melt flow.

pre-heated before the melt transfer. In some experiments an electrically heated cover was installed on top of the launder. The melt temperature was controlled at the pouring point and at the launder outlet by a K-thermocouple, and was typically between 750 and 700 °C, respectively.

Experiments were also performed in batch operation when the similar amount of melt was processed in the compartment similar in size to the degassing chamber.

For comparison some acoustic (for water) and gas measurement (for liquid Al) were taken upon ultrasonic processing with a conventional cylindrical sonotrode placed in the degassing chamber (for liquid aluminum) or in a similar in dimensions glass compartment (for water) and submerged 10 mm from the top the melt. The parameters of the ultrasonic processing were kept similar to the experiment with the plate sonotrode. In this case, the tip of the cavitometer probe was placed about 20 mm from the tip of the sonotrode.

3. Results and discussion

3.1. Wavelength assessment

We started with the assessment of wave characteristics of a thin plate. Although an analysis of the vibration of a thin plate fixed at one side is a complicated matter that we are not going to tackle in this paper, Kitaigorodsky and Yakhimovich (1982) and later Hambric (2006) offer a rather simple analytical assessment of the flexural wavelength. The flexural wave speed in a thin plate of thickness h can be calculated as:

$$C_f = \left(\frac{D\omega}{\rho h}\right)^{\frac{1}{4}}, \quad (1)$$

where D is the flexural rigidity calculated as

$$D = \frac{Eh^3}{12(1-\mu^2)}, \quad (2)$$

where $\omega = 2\pi f$ is the angular frequency, f is the driving frequency, ρ is the plate material density, h is the plate thickness, E is Young's modulus of the plate material, and μ is Poisson's ratio.

The wavelength is then calculated as

$$\lambda = C_f/f. \quad (3)$$

Using the data of our vibratory system and Ti properties summarized is Table 1, we arrive at a wavelength of 33 mm.

3.2. Acoustic measurements

The measurement of the vibrational amplitude showed the following. The vibrational frequency of the transducer was 17.15 kHz. At this frequency and 3.5–4 kW power of the generator, the null-to-peak amplitude at the tip of the steel extension (where the plate was connected) was 11–12 μm as measured by the contactless vibrometer. Along the Ti plate the amplitude varied according to the wavelength of the flexural vibrations from 1 μm in the nodes to 18–25 μm in the antinodes. The distance between the nodes and antinodes was about 6–8 mm, which is in good agreement with the quarter wavelength of the flexural wave.

It is known that the cavitation threshold in water and liquid Al corresponds to the null-peak amplitudes of about 2.5 and 5 μm, respectively, at 20 kHz (Komarov et al., 2012). Therefore the measured amplitudes (18–25 μm) should be enough to achieve the cavitation condition in the melt, which is an important condition for ultrasonic degassing.

A rather simple but vivid test for cavitation activity can be done by placing a thin foil in the cavitation region. Cavitating and imploding bubbles will cause damage of the foil, testifying for the presence of cavitation. A 10-μm thick aluminum foil was fixed on a steel wire frame and placed 5 mm above the plate sonotrode submerged in water. The ultrasonic processing then started and continued for 30 s. The results are shown in Fig. 2. The cavitation damage is clearly seen. It is also obvious that this damage follows a periodic pattern corresponding to the half wavelength of the flexural wave. The measurement shows a spacing of 14–15 mm, which is remarkably close to the analytically obtained value of 16.5 mm (see the wavelength in Table 1). Note that the wavelength may change in the presence of a load, e.g., water or liquid aluminum.

These values are also close to the experimentally measured half-wavelengths in a Nb plate (12 mm at 18 kHz (Eskin, 2002)) and in a stainless steel plate (15 mm at 20 kHz (Shoh, 1976)). The differences are due to the acoustic properties of the material and the operation frequency.

In the next stage, we performed acoustic measurements for cylindrical and plate sonotrode in water and the liquid aluminum alloy.

Tests in water and liquid Al were performed using a Ti plate sonotrode attached to the tip of the steel extension. The plate was submerged inside the liquid melt at a distance of 50 mm from its free surface and equally from the bottom of the vessel similar in dimensions to the degassing chamber. A high temperature cavitometer device calibrated to measure acoustic pressures in liquid

Table 1
Titanium plate characteristics and the results of acoustic calculations.

h (mm)	E (GPa)	μ	ρ (kg/m^3)	f (kHz)	D (kg m^2/s^2)	C_f (m/s)	λ (mm)
2	116	0.32	4507	17.15	86.15	576	33

environments up to 750 °C was deployed. The tip of the cavitometer was submerged within the liquid in a distance of about 15 mm from the surface of the Ti plate. The melt temperature during the experiment with liquid Al was decreasing from 720 to 665 °C upon a series of measurements that were repeated at least three times for each point along the longitudinal axis of the plate sonotrode. In experiments with water the room temperature was maintained. Similar measurements were performed with a cylindrical sonotrode submerged 10 mm below the liquid surface. In this case, the measurements were taken at about 20 mm below the sonotrode.

Typical acoustic spectra are shown in Fig. 3. The driving frequency measured by the cavitometer as 17.15 kHz was in a good agreement with the indicator on the magnetostrictive transducer controller. Note that the shape of the spectrum with the humps in specific frequency domains, i.e., from 170 to 270 kHz in Fig. 3, is attributable to the variation in the sensitivity response of the cavitometer sensor. Also the acquisition rate for measurement in the liquid aluminum alloy was lower than for water (resolution bandwidth of 380 Hz).

Hodnett et al. (2004) gives some features of such spectra that are indicative of the cavitation behavior. There is a well-pronounced peak at the driving or fundamental frequency (17.15 kHz) that is produced by the acoustic field generated by the sonotrode as well as by the intensity from the superimposed linear bubble oscillations. There are also further peaks that are integer multiples of the fundamental frequency (harmonics), which result from non-linear bubble oscillations. The non-linear oscillations of larger bubbles cause their splitting and high-energetic oscillations of smaller bubbles at higher frequencies, which according to Eisner et al. (2013) is displayed by large and sharp peaks in the frequency spectrum. The harmonics, i.e., the 2nd harmonic in Fig. 3a and b (shown by arrow), in some cases can be higher than the fundamental frequency as acoustic emissions from linear (non-inertial) behavior of the cavitation bubbles are superimposed, increasing the strength and sharpness of the signal. At frequencies below the driving frequency, there are so-called subharmonics (fractions of the fundamental frequency) that are indicators of the inertial cavitation activity of larger and longer-lived bubbles (shown by arrows in Fig. 3). Multiple peaks between the harmonics are produced by cavitation activity of bubbles. And, finally, the general level of the noise (broadband signal) is generated by the shock waves of collapsing bubbles as well as by the stable or transient activity of the bubbles in a wide range of sizes, and therefore can be considered as a characteristic of overall cavitation development and activity. The borders of the various regions in the spectrum as well as the sharpness of the peaks can be used for the assessment of the minimum and maximum bubble sizes and the characterization of the cavitation regime (stable/transient).

Although the shapes of the spectra in Fig. 3a and b are similar, the prominent peaks are much sharper in the case where the cylindrical sonotrode was deployed (Fig. 3b). This means that there are more cavitation events in the measured area in the case of the cylindrical sonotrode, but this also means that the cavitation intensity may be distributed over the larger area in the case of the plate. Another difference between these two spectra is that the noise level in the range above 140 kHz (this frequency range is associated with activity from cavitation bubbles) is higher in the case of the cylindrical sonotrode (one should look at the upper edges of the peaks and take into account that the scale is negative so −50 dBu is larger than −60 dBu). This is due to the severity of cavitation collapses and the number of cavitation events. The rise in the broadband at frequencies above 140 kHz is an indication of inertia (transient) cavitation while the rise in the peak levels is related with stable (non-inertial) non-linear cavitation and the number of cavitation events. Thus in Fig. 3a, the stable cavitation possibly prevails compared to Fig. 3b where a more chaotic cavitation environment is developed. This is well explained by Yasui et al. (2011) who showed that the driving amplitude (static pressure) can be a decisive parameter for the performance of bubbles in a sonicated liquid. If the amplitude is at lower levels, bubbles are likely to pulsate for a longer periods of time without collapsing and eventually

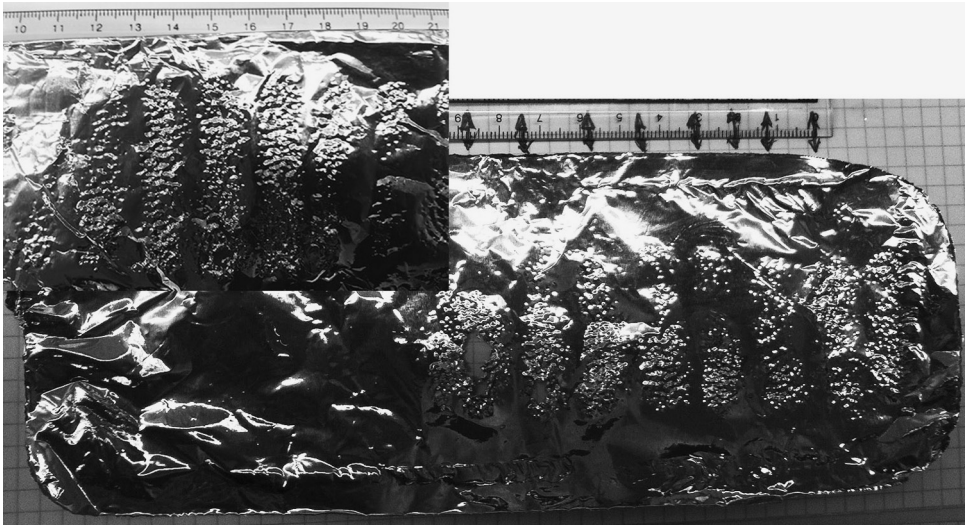

Fig. 2. Aluminum foils showing the regular cavitation damage from a plate sonotrode in water (a ruler shows the regularity of the damage with about 14–15 mm spacing). Insert shows the repeatability of the results.

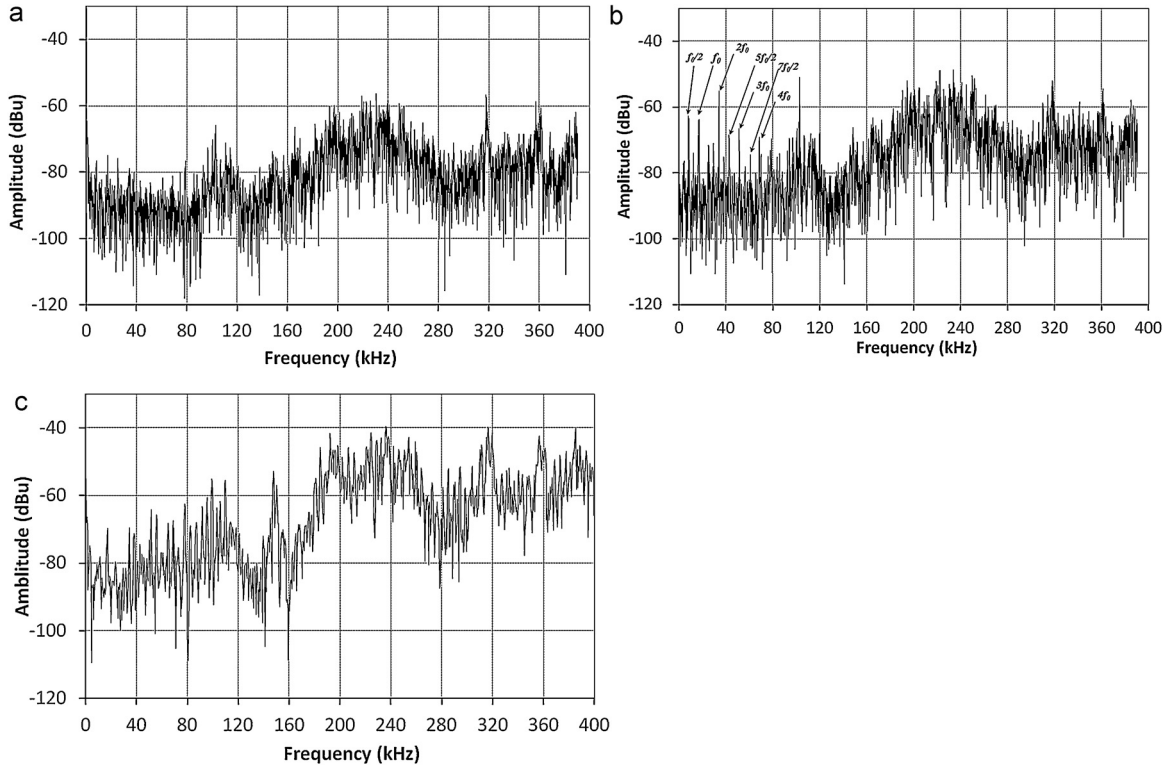

Fig. 3. Examples of typical acoustic spectra measured using a high temperature cavitometer in (a) in distilled water with a plate sonotrode; (b) in distilled water with a cylindrical sonotrode; and (c) in liquid aluminum A356 alloy using a plate sonotrode (generator power 3.5 kW, 17.15 kHz, amplitude at the cylindrical concentrator/sonotrode tip 12.5 μm null-peak). Arrows in (b) show harmonics (nf_0), sub- (f_0/n) and ultra-harmonics (nf_0/p), where n and p are integers.

move toward the free surface promoting degassing. In contrast, when the amplitude increases, collapse events become regular leading the bubbles to chaotic implosions rather than to direct degassing.

We can conclude that the cavitation development is quite prominent in both cases (plate and cylindrical sonotrodes). However, in the case of the plate sonotrode the cavitation events are spread over a larger area and cavitation may be sustained in a more stable way (more bubbles oscillate than collapse).

In the case of the liquid aluminum alloy in Fig. 3c, the acoustic spectrum shows the same main features and the spectra obtained in water. There are subharmonics and prominent ultraharmonics indicative of cavitation development. The noise level is higher than in water (−40 dBu, which is 100 times larger than −60 dBu in the case of the plate in water, as the dBu scale is logarithmic), which may mean more cavitation activity and acoustic pressure. This is because of the higher values of physical parameters of the aluminum melt compared to water, i.e., density, viscosity, surface tension, which may result in more cavitation activity and acoustic pressure.

The intensity of acoustic signal can be recalculated to root mean square (RMS) acoustic pressure as shown in Fig. 4. The measurements were taken at equal distances along the plate longitudinal axis, but not in the exact locations of nodes or antinodes as those may shift under loading with liquid aluminum as compared with those determined experimentally in air or water. The measured acoustic pressure represents a volume and time averaged value and does not vary much with the position of the measurement.

The measured pressure values are in a good agreement with the acoustic pressures at about 3 cm from the tip of a cylindrical sonotrode working in a crucible filled with molten aluminum and excited by the same magnetostrictive device (Tzanakis et al., 2015b). The reason for relatively low values of acoustic pressure is due to the attenuation of the acoustic signals received by the cavitometer as the sound travels from the active cavitation zone to the tip of the cavitometer.

Assuming that inside the crucible where only the cylindrical sonotrode was operating at full power the cavitation phenomena were developed (as can be justified by the noise produced and the spectrum analysis, and other phenomena such as degassing (Eskin et al., 2015)); the acoustic emissions at similar to the “crucible” levels should imply that cavitation activity is also taking place in the degassing chamber with the plate sonorode.

Fig. 4 also shows a definite effect of melt temperature on the ultrasound emission intensity with larger acoustic pressure measured at lower temperatures. Specifically, acoustic pressures are about two times higher on average while increasing up to five times toward the end of the plate. An explanation can be found in the fact that when molten Al approaches its liquidus temperature, hydrogen that is dissolved in the melt is released so more bubbles are initiated giving more cavitation collapsing events. It is the same mechanism as in water (albeit with the temperature increase) when a higher temperature makes the formation of air bubbles easier due to higher levels of vapor pressure. This is particularly pronounced at the end of the plate where due to the geometrical features of the equipment the amplitude is higher forcing the bubbles to collapse more frequently.

After confirming that the cavitation conditions are met by the suggested scheme of ultrasonication, the experiments for melt degassing were performed.

3.3. Ultrasonic degassing of aluminum melt

The ultrasonic degassing was first tried in a batch operation where a compartment similar in size to the degassing chamber

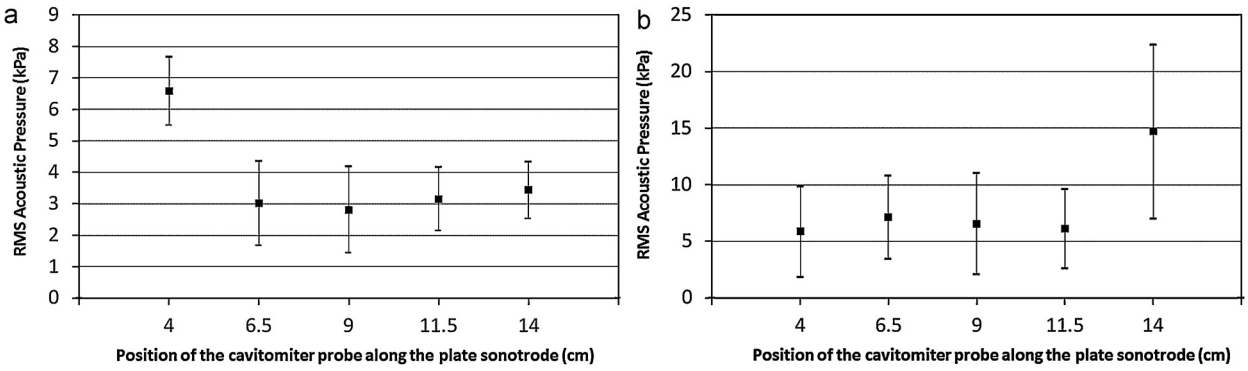

Fig. 4. Characterization of the RMS acoustic pressure field inside the degassing chamber with a liquid A356 alloy generated by the Ti plate sonotrode at various positions of the cavitometer along the plate surface (from the bend toward the edge (see Fig. 1): (a) data for 720–700 °C and (b) data for 690–670 °C. The average point is for 30 measurements with their standard deviation values illustrated by the extended bars.

Table 2
Results of ultrasonic degassing in batch operation using different methods of ultrasonication.

Degassing method	Ambient humidity (%)	Density index before degassing (%)	Density index after degassing (%)	H_2 (cm^3/100 g) before degassing	H_2 (cm^3/100 g) after degassing	Degassing efficiency (%)
Natural	67	15.7	16.3	0.22	0.23	−4.5
Natural	81	20.2	20.0	0.36	0.35	2.8
Cylindrical sonotrode	67	20.3	14.7	0.36	0.195	45.8
Cylindrical sonotrode	67	14.9	7.3	0.2	0.1	50
Plate sonotrode[a]	64	24.5	7.4	0.53	0.09	83
Plate sonotrode	67	22.45	9.24	0.44	0.11	75
Plate sonotrode	81	19.0	7.25	0.31	0.09	70.9
Plate sonotrode[a]	81	27.3	13.7	0.66	0.17	74.2

[a] Melt temperature in the furnace was 800 °C.

Table 3
Results of ultrasonic degassing using the plate sonotrode in the melt flow.

Amount of melt degassed (kg)	Ambient humidity (%)	Density index before degassing (%)	Density index after degassing	H_2 before degassing (cm^3/100 g)	H_2 after degassing (cm^3/100 g)	Degassing efficiency (%)
18 (no sonication)	60	17.2	17.8	0.26	0.28	−7.7
18	61	17.3	12.1	0.26	0.15	42.3
18	86	22	15.7	0.42	0.22	47.6
25	65	22.9	15.5	0.46	0.21	54.3

was used. In this case the comparison was made between the cylindrical sonotrode submerged from the top of the melt (conventional scheme of degassing) and the plate sonotrode located in the lower third of the melt volume. The treated melt weight was 5.7 kg, melt temperature 750 °C (if not mentioned otherwise), sonication time 2 min and resting time 4 min. The results are shown in Table 2 in comparison with "natural" degassing, when the same amount of melt was staying in the same vessel for the same amount of time (6 min), with the submerged but idle plate sonotrode. This experiment was performed to avoid confusion with some statements that natural degassing can be as efficient as forced degassing (Campbell, 1993). Note that in our experiments natural degassing does not produced any significant decrease in the hydrogen concentration, and can actually result in some hydrogen pick-up from the atmosphere.

These results confirmed our initial idea that the larger surface area of the plate sonotrode that emits cavitation bubbles in several locations and directs them upwards in the melt, increases the efficiency of ultrasonic degassing. In the performed experiments the efficiency of degassing with the plate sonotrode was about 25% greater than with the cylindrical sonotrode (about 50% improvement). One can also see that the increased ambient humidity and melt temperature, although change the hydrogen solubility, do not affect significantly the efficiency of ultrasonic degassing. A slight improvement of degassing efficiency (but not the final hydrogen concentration) for the melt superheated to 800 °C is related to a higher starting concentration of hydrogen, due to the higher hydrogen solubility at the higher temperature. It is known that the efficiency of the ultrasonic degassing is the higher, the greater the initial hydrogen concentration is (Eskin and Eskin, 2014).

Next, the plate sonotrode was used for ultrasonic degassing in the melt flow according to the scheme shown in Fig. 1a. The melt flow rate was 3.3 kg/min, which allowed the melt to have about 2 min of residence time in the degassing chamber. The amount of the melt in the degassing chamber was similar to the batch operation, whereas the total amount of degassed metal was either 18 or 25 kg. The results are given in Table 3.

The degassing performance of the plate sonotrode is quite good, allowing for about 50% of degassing efficiency, which is quite acceptable by industrial standards.

Further research is needed on the optimization of the melt flow and geometry of the plate sonotrode (thickness, shape, length), which will allow upscaling of this laboratory trials to the pilot scale.

4. Conclusions

(1) A new scheme of ultrasonic melt processing with a plate sonotrode was studied using acoustic measurements in water and a liquid aluminum alloy, and during aluminum melt degassing experiments.

(2) The experimental results on flexural wave propagation in the plate agree well with analytical assessment. The measured null-to-peak amplitudes 18–25 μm at a frequency of 17.15 kHz should be sufficient for developed cavitation in a liquid phase, which is confirmed by the cavitation damage of an aluminum foil in water.
(3) Acoustic measurements of frequency spectra and acoustic pressures show that the suggested scheme allows for the cavitation of the liquid phase (water or Al melt) under conditions favoring stable cavitation.
(4) The feasibility of using the suggested scheme for continuous ultrasonic melt degassing in the flow is clearly demonstrated with the achieved degassing efficiency of 50% (75% for batch operation).

Acknowledgments

The research leading to these results has received funding from the European Union's Seventh Framework Program managed by REA – Research Executive Agency (FP7/2007–2013) under Grant Agreement number 606090 (www.doshormat.eu). I. Tzanakis is grateful to the UK Engineering and Physical Sciences Research Council (EPSRC) for financial assistance in this research under contract number EP/K005804/1.

References

Campbell, J., 1993. Castings, second revised ed. Butterworth-Heinemann, Oxford (UK).
Davies, J.R. (Ed.), 1993. ASM Specialty Handbook. Aluminum and Aluminum Alloys, ASM International, Metals Park, pp. 204–206.
Eisner, J., Schneider, J., Cairos, C., Mettin, R., 2013. Sound films of acoustic cavitation , Proc. the 40th Italian (AIA) Annual F Conf. on Acoustics and the 39th German Annual F Conf. on Acoustics (DAGA), 18–21 March 2013, Merano, Italy. Deutsche Gesellschaft für Akustik, Berlin, pp. 485–488.
Eskin, D., Alba-Baena, N., Pabel, T., da Silva, M., 2015. Ultrasonic degassing of aluminium alloys: basic studies and practical implementation. Mater. Sci. Technol. 31, 79–84.
Eskin, G.I., 1965. Ultrasonic Treatment of Molten Aluminum. Metallurgiya, Moscow.
Eskin, G.I., 1995. Cavitation mechanism of ultrasonic melt degassing. Ultrason. Sonochem. 2, 137–141.
Eskin, G.I., 2002. Device for ultrasonic treatment of light alloy melt. Russian Patent RU2186147, July 27, 2002.
Eskin, G.I., Eskin, D.G., 2014. Ultrasonic Treatment of Light Alloy Melts, second ed. CRC Press, Boca Raton.
Hambric, S.A., 2006. Structural acoustics tutorial—part 1: vibrations in structures. Acoust. Today 2 (4), 21–32.
Hodnett, M., Chow, R., Zeqiri, B., 2004. High-frequency acoustic emissions generated by a 20 kHz sonochemical horn processor detected using a novel broadband acoustic sensor: a preliminary study. Ultrason. Sonochem. 11, 441–454.
Kapustina, O.A., 1970. Degassing of liquids. In: Rozenberg, L.D. (Ed.), Physical Principles of Ultrasonic Technology. Nauka, Moscow, pp. 253–336 (Translated by Plenum, New York, 1973).
Kitaigorodsky, Yu.I., Yakhimovich, D.F., 1982. Engineering Calculation of Ultrasonic Oscillation Systems. Mashinostroenie, Moscow, pp. 14–19.
Komarov, S., Oda, K., Ishiwata, Y., Dezhkunov, N., 2012. Characterization of acoustic cavitation in water and molten aluminum alloy. Ultrason. Sonochem. 20, 754–761.
Shoh, A., 1976. Sonic apparatus. United State Patent 3945618, March 23, 1976.
Tzanakis, I., Hodnett, M., Lebon, G.S.B., Dezhkunov, N.V., Eskin, D.G., 2015a. Calibration and performance assessment of an innovative high-temperature cavitometer. Ultrason. Sonochem. (under review).
Tzanakis, I., Hodnett, M., Lebon, G.S.B., Eskin, D.G., Pericleous, K., 2015b. Direct measurement of acoustic pressure in water and liquid aluminium during ultrasonic processing. Scr. Mater. (under review).
Waite, P.D., 1998. Improved metallurgical understanding of the Alcan compact degasser after two years of industrial implementation in aluminum casting plants. In: Welch, D. (Ed.), Light Metals 1998. TMS, Warrendale (PA), pp. 791–796.
Yasui, K., Towata, A., Tuziuti, T., Kozuka, T., Kato, K., 2011. Effect of static pressure on acoustic energy radiated by cavitation bubbles in viscous liquids under ultrasound. J. Acoust. Soc. Am. 130, 3233–3242.